GENERALIZED INVERSE BEAMFORMING INVESTIGATION AND HYBRID ESTIMATION

P.A.G. Zavala[1], W. De Roeck[1], K. Janssens[2], J.R.F. Arruda[3], P. Sas[1], W. Desmet[1]

[1]Katholieke Universiteit Leuven, Celestijnenlaan 300B, B-3001 Leuven, Belgium

Email: PauloAlexandre.ZavalaGalarce@mech.kuleuven.be

[2]LMS Engineering, Interleuvenlaan 68, 3001 Leuven, Belgium

[3]UNICAMP, R. Mendeleiev 200, PB 6122 CEP 13083970 Campinas-SP, Brazil

ABSTRACT

Conventional beamforming, among the several techniques that can be used for noise source localization, has been widely used in complex problems, including aeroacoustics applications. The sound generated by flow turbulence can present a distributed coherent source region, which presents some challenges to the conventional beamforming localization accuracy. The Generalized Inverse Beamforming (GIB) is a recent method aiming at the identification of coherent or incoherent, distributed or compact, monopole or multipole sources. This method is based on the microphone array cross-spectral eigenstructure, resulting in a robust localization technique. In this work, the performance of the GIB method is investigated for two simple cases in comparison to conventional beamforming. The first test case, a simple monopole, illustrates the frequency range accuracy, and the second test case, two monopoles in coherent radiation, illustrates the different performance in coherent scenarios. Numerical investigation is used to define the test array aperture and distance to the target region. In order to improve the generalized inverse estimation on the coherent case, a new hybrid estimation is proposed. This consists in creating a source mapping that is comparable to the conventional mapping based on the generalized inverse mapping and the array Point Spread Function. The offsetting between the hybrid mapping and the conventional mapping indicates the quality of the generalized inverse estimation and the hybrid estimation points to the actual sources overall strength.

1 INTRODUCTION

Conventional beamforming is the current primary tool for noise source localization in several fields of engineering. Its principle, sum & delay, is of easy understanding, and is a natural basis for other techniques development. Countless methods have been proposed in recent years to address more complex problems, as found, for example, in aeroacoustics applications.

One of the challenges in aeroacoustic problems, is that the source is distributed in coherent regions, demanding a method with a high accuracy for this kind of scenario. Some examples of methods can be found in [1], [2], and [3], using near-field acoustic holography, cross-spectrum based azimuthal decomposition, and robust adaptive beamforming, respectively. These works have some characteristics in common, for example, they were applied to a jet problem at low Mach number, they use an approximately stationary condition for the testing, and they search for the source location and type identification. All these methods still present a low resolution in terms of source center localization.

The recently developed method, Generalized Inverse Beamforming [4] is a promissing alternative to address the several challenges on complex problems. It aims at identifying sources of compact or distributed nature, coherent or incoherent, with monopole or multipole radiation patterns, simultaneously or not. This present a large range of possible applications, and its concepts allows further developments on top of the original algorithm.

This work is a preliminary investigation in regards of two characteristics: The frequency range for a monopole identification; and the localization accuracy for two compact sources in coherent radiation. The results are presented for the generalized inverse beamforming and the conventional beamforming [5]. In the end, a hybrid approach is proposed to illustrate the correspondence between the generalized inverse beamforming and the conventional beamforming. The hybrid estimation gives a secondary estimation that can be used to assess the quality of the generalized inverse beamforming.

2 GENERALIZED INVERSE BEAMFORMING OVERVIEW

The generalized inverse beamforming uses the same array information as normally used in conventional beamforming. The array cross-spectrum data can be arranged in matrix form, leading to the cross-spectral matrix, R. The generalized inverse beamforming is based on the eigen-structure of this response matrix. The decomposition can be described as below:

$$R = U\Lambda U^{\dagger}\,, \tag{1}$$

where U is the eigenvector matrix, Λ is the diagonal matrix containing the eigenvalues, and $U^{\dagger}$ is the complex conjugate transpose of U.

This approach, eigen-decomposition of the cross-spectral method was first derived by Schmidt [6], leading to a range of new methods, such as, MUSIC methods (Multiple Signal Classification). The general interpretation of the eigen-structure is simple, the number of eigen-values represent the number of incoherent source distributions present in the array response, and each eigen-vector, represent the respective response phase relationship. The eigen-value is related to the source strength according to [7]. If the number of microphones is bigger than the number of incoherent sources, the remaining eigen-values are related to the incoherent noise structures.

With the number of eigen-pairs that represents the source structures that are interesting for identification, the response eigen-mode is defined as:

$$v_i = \sqrt{\lambda_i} u_i \,, \tag{2}$$

where v_i is the eigenmode, λ_i and u_i are the corresponding eigenvalue and eigenvector.

On the generalized inverse beamforming, the source localization problem is formulated as finding the source vector, a, that solves the following source/transfer-path/receiver equation using a least squares approach:

$$A a_i = v_i \,, \tag{3}$$

where A is the transfer matrix, containing the radiation patterns from each target grid point to every sensor position. The transfer matrix used in this work consist of monopole radiation [8], but the extension to other radiation patterns, e.g. dipoles, is straightforward to obtain.

The generalized inverse, or pseudo-inverse, equations are used to calculate the source vector, a_i. When a larger number of target grid points than sensors is used, an underdetermined system is obtained and the following equation can be used:

$$a_i \approx A^\dagger (A A^\dagger)^{-1} v_i \,. \tag{4}$$

In the case of an overdetermined system, the following equation can be used:

$$a_i \approx (A^\dagger A)^{-1} A^\dagger v_i \,. \tag{5}$$

Since the matrix $AA^\dagger$ is generally ill-conditioned, a Tikhonov regularization is used [4] to solve equation (4) or (5). This introduces an artificial diagonal term on this matrix, resulting in the following equations for, respectively, the underdetermined and the overdetermined system:

$$a_i \approx A^\dagger (A A^\dagger + \alpha^2 I)^{-1} v_i \,, \tag{6}$$

$$a_i \approx (A^\dagger A + \alpha^2 I)^{-1} A^\dagger v_i \,, \tag{7}$$

where α is the Tikhonov regularization factor, and I is the Identity matrix.

The Tikhonov regularization corresponds to the minimization of the following cost function:

$$J_2 \equiv ||a_i||^2 + \alpha^{-2} ||v_i - A a_i||^2 \,, \tag{8}$$

where $||.||$ is the Euclidean norm.

In the original method presentation [4], the square of the regularization factor is chosen as a fraction of the greatest eigenvalue of the matrix $AA^\dagger$, with suggested range from 0.1% to 5%.

The estimation is calculated by summing the source vector terms related to each coherent mode. However, the solution brought by equations (6) and (7) are least squares approximations, and this approach is not accurate, since distributed sources will have their contributions squared and then summed. To illustrate this characteristic, consider a unitary source retrieved by two grid points, the source vector summation using a 2-norm approach is $(1/2)^2 + (1/2)^2 = 1/2$, which results in an incorrect total. The overall strength of the source vector is more accurately calculated using 1-norm, $(1/2) + (1/2) = 1$.

For this reason, it is suggested to redefine the source detection problem as a minimization of the following cost function [4]:

$$J_1 \equiv |a_i| + \alpha^{-2}|v_i - Aa_i|^2 \,, \tag{9}$$

where $|.|$ is the 1-norm, representing the direct summation of the vector terms.

This has the advantage of a more accurate strength estimation for distributed sources. Since no direct approach can be adopted to solve this minimization problem, the method proposed by Susuki [4] searches the minimum of the cost function iteratively, truncating the source vector on each iteration, discarding the irrelevant target grid points, and using the least squares equations to recalculate the source vector. This process is applied until a predefined criteria is fulfilled, for example, a minimum number of remaining terms in the source vector. A simplified version of the algorithm can then be described as:

1. Calculate the initial source vector, a, using the generalized inverse equations (6) or (7);
2. Reorder and truncate (10%) the source vector, discarding the smallest terms;
3. Calculate a new source vector, using equations (6) or (7);
4. Repeat item 2 and 3 until a defined number of source terms is reached;
5. Apply Gaussian spatial filter on the final mappings.

The use of a spatial Gaussian filter on the final mappings has the mere purpose of improving the mapping visualization, since the estimated strength remains unchanged.

3 MONOPOLE AT ORIGIN

This first example is used to illustrate the performance in identification in terms of frequency range. But first, numerical tests are used to define the appropriate array configuration in terms of aperture and distance to the target plane. The array configuration is a 6-arm spiral layout, similar to the array used on [4], but with 30 microphones. The target grid points distribution adopted in this work is similar to what is adopted in [4] for the numerical models tests, target grid range is 6 wavelengths, and spacing is $1/4$ of a wavelength. The generalized inverse algorithm is stopped after the source vector reaches a minimum size of 21 terms. All results are average of 5 estimations. Estimations used signal blocks with 1024 samples.

The numerical tests for a unitary strength 1kHz monopole source in free-field located at the target grid center, varying the array aperture and distance to target, is shown in table 1. The source signal included noisy according to the same strategy used by Susuki in [4], but with a factor of 0.5 to have a less aggressive noise and comparable to what is found in the experiments. The sampling frequency covered 10 wavelengths per block.

According to the results, good estimates (with error less than 10%) are found with ratio between the distance to the aperture starting around on 1. It is clear from the results, that estimates can be done as close as 1 wavelength, and in general, ratios above 1 generates good estimates. For convenience, the ratio for the experiments was chosen to 1.25, and tests done with spiral at 2.5m distance to the source, and aperture diameter of 2m. The chosen microphones positioning and test configuration for the monopole testing can be observed in figures 1a and 1b, respectively.

Table 1: *Estimations varying array distance and aperture.*

		Distance to Target in wavelengths						
		1	2	5	10	15	20	50
Aperture in wavelengths	1	1.05	1.00	0.96	0.96	0.96	0.96	0.96
	2	1.18	1.02	0.98	0.96	0.96	0.95	0.95
	4	1.69	1.36	1.00	0.99	0.97	0.96	0.96
	6	1.77	1.55	0.99	0.99	0.98	0.97	0.96
	8	1.83	1.51	1.26	0.99	0.99	0.98	0.96
	10	1.82	1.60	1.40	1.00	0.99	0.98	0.96
	12	1.74	1.72	1.49	1.02	1.00	0.99	0.96
	14	1.80	1.71	1.47	1.09	1.01	0.99	0.97

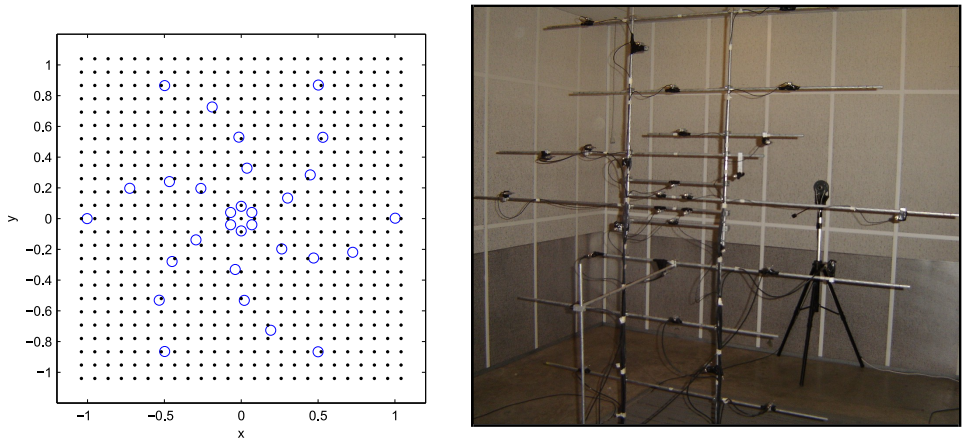

(a) (b)

Figure 1: *(a) Microphones positioning (circles) and target grid points (dots) [m]; (b) Experimental layout: Microphone array; and compact source.*

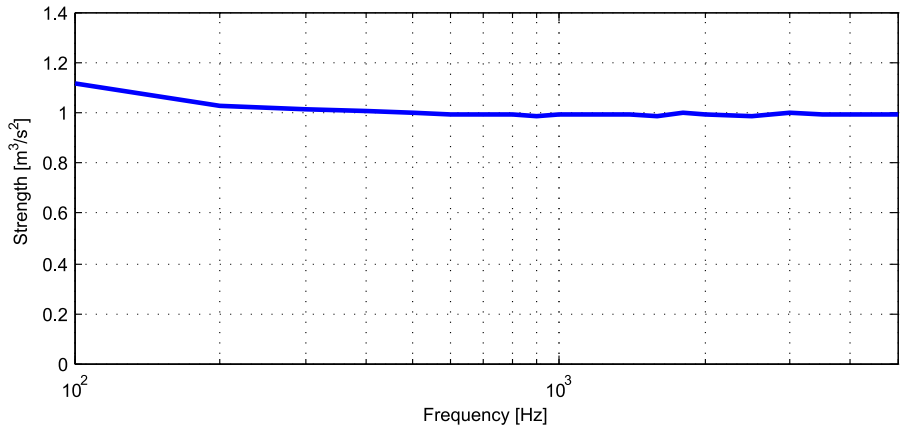

Figure 2: *Estimations varying radiation frequency for a unitary monopole source.*

For the chosen configuration, numerical tests are performed varying the source frequency, from 100Hz to 5kHz. The results are presented on figure 2.

Estimations above 100Hz are expected to have more accurate results, with error smaller than 10%, according to the numerical simulations. This result already demonstrates the broad frequency range of this method, the generalized inverse beamforming.

Three frequencies are chosen for the experiments. The source mappings for a unitary source at 200Hz, 1kHz, and 5kHz, are presented, respectively, in figures, 3, 4, and 5, for conventional beamforming and the generalized inverse beamforming methods. Acquisition uses 20.48kHz sampling rate for the 200 and 1kHz tests, and 102.4kHz for the 5kHz test.

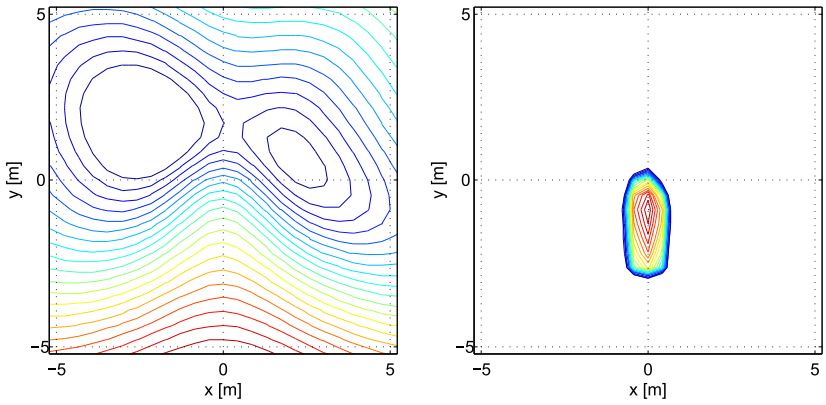

Figure 3: *Monopole with 200Hz radiation: (a) Conventional beamforming (b) Generalized inverse beamforming (contour lines are in 10 dB range with 0.5 dB increment).*

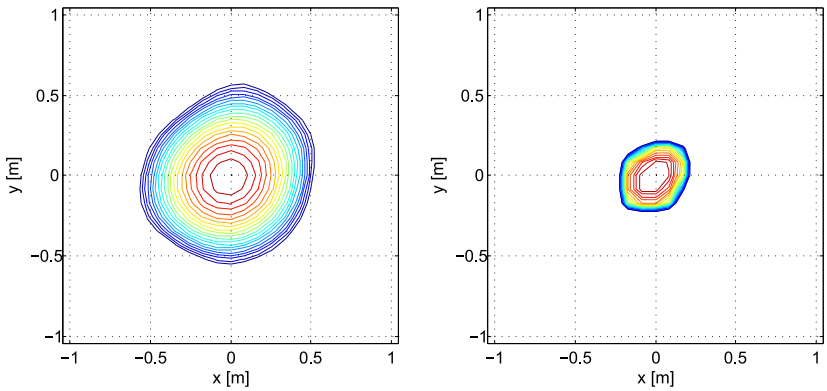

Figure 4: *Monopole with 1kHz radiation: (a) Conventional beamforming (b) Generalized inverse beamforming (contour lines are in 10 dB range with 0.5 dB increment).*

From the results, is observed that the conventional beamforming is not capable to locate source at 200Hz, while the generalized inverse beamforming produces a mixed identification with the reflections on the floor, considering that the source was located at approximately 1.6m from the ground.

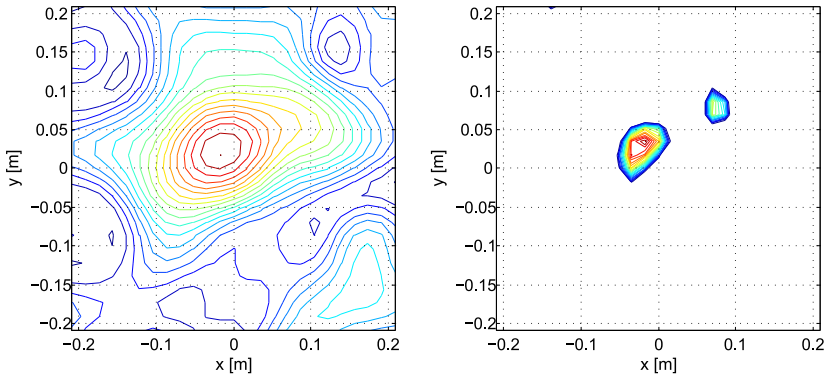

Figure 5: *Monopole with 5kHz radiation: (a) Conventional beamforming (b) Generalized inverse beamforming (contour lines are in 10 dB range with 0.5 dB increment).*

For the 1kHz result, it is clear the advantage of the generalized inverse beamforming in dynamic range, presenting the source location with 10dB range with around $1/2$ wavelength radius, compared to the conventional beamforming result of around 1 wavelength radius.

For the 5kHz source radiation case, both methods present a source center, but the higher dynamic range for the generalized inverse beamforming is also clear. Both results indicate a small offset for the source center, and this is attributed to the array positioning errors, with estimated offset of about 30mm from the correct location, which is low compared to the test involved dimensions.

The generalized inverse mapping present a spurious peak on the range of 10dB, and this also can be explained by the array positioning error. The expected limitation to go beyond 5kHz is only the array positioning error.

The strength estimations for the conventional beamforming and the generalized inverse beamforming are presented in table 2. The results for the conventional beamforming are calculated at the maximum value on the mapping.

Table 2: *Source strength estimations for three different frequencies.*

Frequency	**Conventional beamforming**	**Generalized inverse beamforming**
200Hz	2.10	1.06
1kHz	1.11	0.92
5kHz	0.63	0.63

The generalized inverse beamforming present more accurate or similar estimations than conventional beamforming for all three tested frequencies. This indicates that the generalized inverse beamforming has a broader frequency range in respect to lower frequencies. For higher frequencies, the indication is that estimations are affected by the same amount of error for both methods. A better microphone positioning accuracy is expected to enhance results for higher frequencies.

4 TWO MONOPOLES IN COHERENT RADIATION

Now, to illustrate the generalized inverse superior performance in coherent scenarios, a simple test using two compact sources separated by two wavelengths is used. The sources are set to radiate in-phase at 1kHz. The array configuration, aperture, distance to target plane, target grid range, and target grid spacing, are all the same as on previous example.

The mappings for the conventional beamforming and generalized inverse beamforming are presented in figure 6.

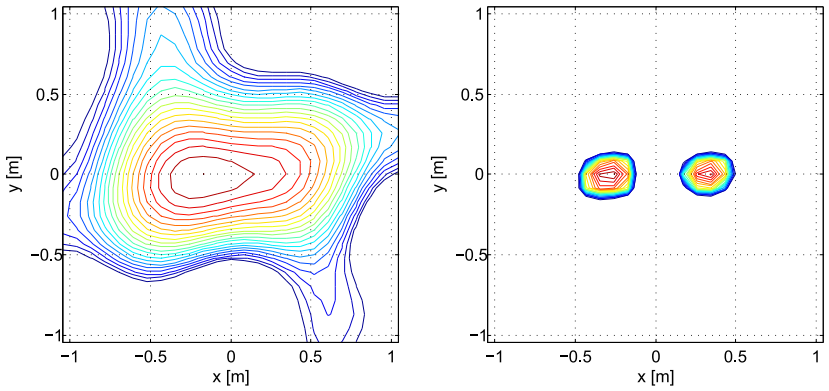

Figure 6: *Two monopoles in-phase with 1kHz radiation: (a) Conventional beamforming (b) Generalized inverse beamforming (contour lines are in 10 dB range with 0.5 dB increment).*

Is clear from the results that the generalized inverse beamforming is capable to identify two monopole sources, and that the conventional beamforming does not present a clear identification. The number of terms on the source vector is still 21 terms, and this leads to a reduced radius than $1/2$ wavelength for the 10dB range, since the 21 terms are now distributed in two sources. The conventional beamforming asymmetric result could be related to the array distribution, with peak closer to the region with more microphones. The estimations are presented on table 3. The conventional beamforming result is obtained at the mapping peak.

Table 3: *Strength estimations for two monopoles in-phase example.*

Frequency	**Conventional beamforming**	**Generalized inverse beamforming**
1kHz	1.26	1.41

The result for the generalized inverse beamforming is the best approximation to the expected response, $q = 2$. But still not accurate enough, and an improved methodology is required.

5 HYBRID ESTIMATION

Conventional beamforming is based on the delay & and sum principle, and can be stated as shown in the equation below:

$$P = w^{\dagger} R w \,, \tag{10}$$

where w is the vector with the weighting factors (or delays).

The estimation retrieved by conventional beamforming is equivalent to a directional microphone with the same dynamic characteristics of the Point Spread Function of the array. The Point Spread Function can be described by the equation below:

$$PSF = |w^{\dagger} w_o|^2 \,, \tag{11}$$

where w_o is the weighting vector related to the point of interest.

The conventional beamforming is a robust estimation technique, with signal to noise ratio improved according to the number of microphones on the array. The hybrid estimation is based in the conversion of the generalized inverse mapping, using the array point spread function, to an equivalent mapping. This process takes advantage of the more accurate source mapping from the generalized inverse method, and the less sensitive to noise conventional mapping. The conversion is described as:

$$P_o = |a_i PSF^{1/2}|^2 \,, \tag{12}$$

where P_o is the power at a particular target grid point.

On figure 7 is shown the original generalized inverse beamforming from the two monopoles in coherent radiation example, and the array Point Spread Function for the grid center.

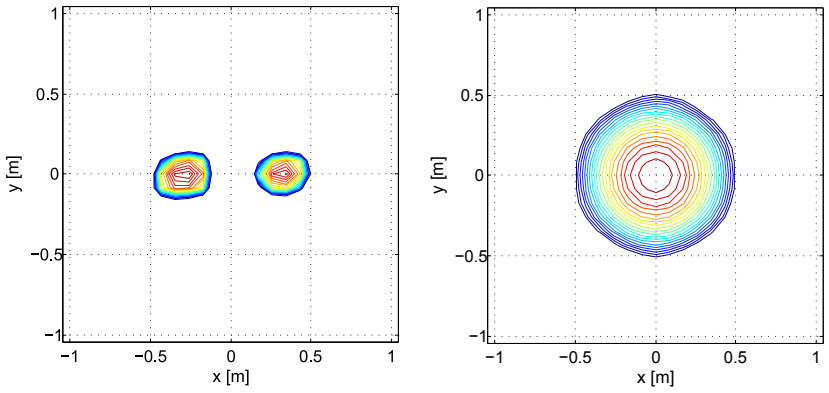

Figure 7: *(a) Two monopoles in-phase with 1kHz radiation, generalized inverse beamforming (b) Array Point Spread Function for the grid center (contour lines are in 10 dB range with 0.5 dB increment).*

This converted mapping, or hybrid mapping, is then compared to the conventional mapping, and the averaged strength offsetting is used to estimate the difference between the two mappings.

In figure 8, the conventional mapping for the two monopoles case and the hybrid mapping is presented.

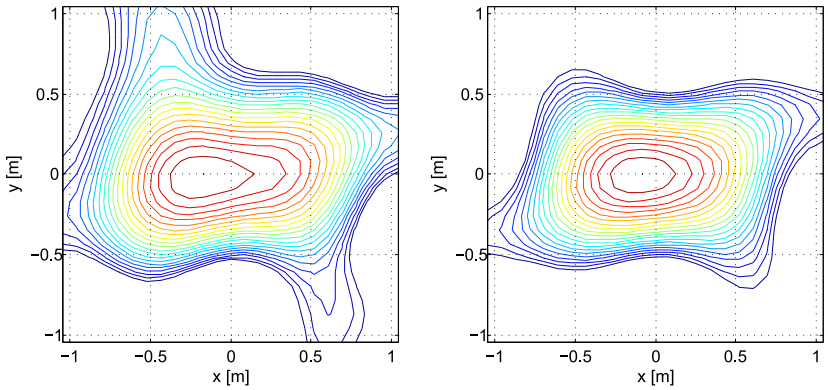

Figure 8: *Two monopoles in-phase with 1kHz radiation: (a) Conventional beamforming (b) Hybrid mapping based on the generalized inverse beamforming (contour lines are in 10 dB range with 0.5 dB increment).*

The similarity between the two mappings is clear from the results. However, since the generalized inverse mapping is a distributed mapping, there is an expected difference from the hybrid mapping to the conventional mapping. This is caused by the point spread function being applied to a distributed source mapping, and the sum over this results is lower than the actual source strength multiplied by the point spread function at the source center location. Or, in other words, if the generalized inverse mapping would be a concentrated source mapping instead of the distributed, the hybrid mapping would be equal to the conventional mapping.

The offsetting between the conventional mapping and the hybrid mapping, when applied to the generalized inverse results, lead to a mapping that is the closest approximation to the original conventional mapping. This offsetting when added to the generalized inverse results, includes the error due to the distributed nature of the generalized inverse beamforming. Causing the hybrid estimation to be an overestimation of the source mapping. The proposal here is that the hybrid offsetting is a limit of probable estimation, and the best approximation would be an intermediate value between the original generalized inverse estimation and the value with added offsetting. On table 4, the generalized inverse estimation, hybrid offsetting and the hybrid estimation estimation, are presented.

Table 4: *Generalized inverse and hybrid estimation for the two monopoles example.*

Generalized inverse beamforming	**Offsetting [%]**	**Hybrid estimation**
1.41	48	2.08

Even considering that the hybrid estimation is closer to the combined source strength, $q = 2$, it has inherent error due to the distributed nature of the generalized inverse mapping. Another aspect is that the conventional beamforming estimation also has some errors related to the presence of noise on the measurements. This two aspects, explains the remaining gap from the hybrid estimation to the actual combined source strength. Taking these aspects into consideration, the hybrid offsetting certainly indicates the quality of the generalized inverse beamforming estimation by comparison to the conventional beamforming, and certainly points to the range of a more accurate estimation.

6 CONCLUSIONS

The investigations used a 6-arm spiral array configuration, and two cases of monopole sources: One monopole at target grid center; and two monopoles in coherent radiation. The first test case is used to illustrate the array characteristics, array aperture and distance to target grid, influence on estimation, and also the frequency range accuracy in estimation and mapping.

Some characteristics can be pointed out from the investigation performed. First, that using the 6-arm spiral configuration, a ratio about one or higher, between the distance from the array to the source target plane, and the array aperture, leads to an accurate monopole source strength estimation. Even with the array as close as one wavelength from the target plane, the generalized inverse method is capable to give an accurate estimation.

The investigation performed also demonstrated the superior performance on frequency range for localization of a compact source, with a broader low frequency range in respect to mapping. This is an important advantage of the generalized inverse method since one of the drawbacks on the conventional beamforming is the restricted low frequency accuracy.

The second test example, two monopoles is coherent radiation, is used to illustrate the higher accuracy on coherent scenarios in locating source centers compared to the conventional beamforming. The higher dynamic range on the generalized inverse method allowed the individual source center detection while the conventional beamforming is not able to locate the individual source centers.

Despite the estimation using the generalized inverse method being already more accurate than the conventional beamforming on the presented case, a new method is applied to the generalized inverse result, and a hybrid estimation between the conventional beamforming method and the generalized inverse method, presented. This hybrid estimation points to the region of a more accurate estimation, and indicates the quality of the original generalized inverse method's result.

These findings confirm the potential of the generalized inverse beamforming method to be used in more complex problems, with advantages such as: broader frequency range; lower array distance limit to region of interest, with respective lower array size; higher spatial accuracy in coherent cases; accurate source strength estimation; and the possibility to apply a less sensitive to noise estimation, the hybrid estimation.

7 ACKNOWLEDGEMENTS

The authors want to acknowledge the financial support given by Marie Curie Fellowships for Early Stage Research Training (SIMVIA II), and the cooperation effort by Katholieke Universiteit Leuven, PMA department, and State University of Campinas (UNICAMP), Computational Mechanics Department. The authors also would like to thank all suggestions and technical discussions conducted with experts from LMS Engineering.

References

[1] M. Lee, J.S. Bolton, L. Mongeau, "*Application of cylindrical near-field acoustical holography to the visualization of aeroacoustic sources*", J. Acoust. Soc. Am. 114 (2), pages: 842-858, August 2003.

[2] V.F. Kopiev, M. Y. Zaitsev, S.A. Velichko, A.N. Kotova, I.V. Belyaev, "*Cross-correlation of far field azimuthal modes in subsonic jet noise*", 14th AIAA/CEAS Aeroacoustics Conference, May 2008-2887.

[3] T. Susuki, "*Identification of multipole noise sources in low Mach number jets near the peak frequency*", J. Acoust. Soc. Am. 119 (6), pages: 3649-3659, June 2006.

[4] T. Susuki, "*Generalized Inverse Beam-forming Algorithm Resolving Coherent/Incoherent, Distributed and Multipole Sources*", 14th AIAA/CEAS Aeroacoustics Conference (29th AIAA Aeroacoustics Conference), paper No. 2954, Vancouver, British Columbia Canada, 5-7 May, 2008.

[5] U. Pillai, "*Array Signal Processing*", Chap. 2, Springer, New York, 1989.

[6] R.O. Schmidt, "*Multiple Emitter Location and Signal Parameter Estimation*", IEEE Trans. on Antennas and Propagation, Vol. AP-34, No. 3, 1986.

[7] T.J. Mueller (Ed.), "*Aeroacoustics Measurements*", Chap. 2 (Chapter Author: R.P. Dougherty), Springer, New York, 2002.

[8] P.M. Morse, "*Vibration and Sound*", Chap. VII, McGraw-Hill, Second Edition, New York, 1948.